Electron Cyclotron Power Losses in Fusion Reactor-Grade Tokamaks: Scaling Laws for Spatial Profile and Total Power Loss

A.B. Kukushkin 1), P.V. Minashin 1,2), V.S. Neverov 1,2)

1) Nuclear Fusion Institute, RRC "Kurchatov Institute", 123182 Moscow, Russia
2) Moscow Engineering Physics Institute, 115409 Moscow, Russia

e-mail contact of A.B. Kukushkin: kuka@nfi.kiae.ru

Abstract. Potential importance of electron cyclotron (EC) wave emission in the local electron power balance in the steady-state regimes of ITER operation suggested analyzing in more detail the accuracy of calculating the 1D distribution, over magnetic flux surfaces, of the net radiated power density, $P_{EC}(\rho)$. Recent comparison of numeric codes SNECTR, CYTRAN, CYNEQ and EXACTEC for different electron temperature profiles and average temperatures of relevance for fusion reactor-grade magnetoplasmas, has shown good agreement of results within two different cases: (A) specular reflection in a circular cylinder (SNECTR, EXACTEC) and (B) diffuse reflection in a circular cylinder (SNECTR), and diffuse reflection in any geometry or any reflection in a noncircular toroid (CYTRAN, CYNEQ). These cases were shown to provide, respectively, the lower and upper bounds for $P_{EC}(\rho)$, including that for the modulus of $P_{EC}(\rho)$, inverted in sign in the plasma column periphery. Here we extend this analysis to show the following approximate scaling laws on the example of calculations with CYNEQ: (i) new formula for the volume-integrated EC power loss, P_{EC}^{tot}, which gives a simplest extension of the Trubnikov's formula, originally suggested for *homogeneous* electron density n_e and temperature T_e, to the case of n_e and T_e profiles expected for ITER and DEMO; (ii) the normalized profiles, $P_{EC}(\rho)/P_{EC}^{tot}$, for identical normalized temperature profiles, $T_e(\rho)/<T_e>$, appear to be very close for substantially different volume-averaged temperatures, $<T_e>$; (iii) in the central plasma, profile $P_{EC}(\rho)$ in the case A may be close enough to that in the case B for larger value of wall reflectivity R_w, thus depending on an effective R_w, incorporating the type of reflection (diffusive or specular) and the geometry of the vacuum chamber.

1. Introduction

Potential importance [1] of electron cyclotron (EC) wave emission in the local electron power balance in the steady-state regimes of ITER operation suggested the necessity to analyze in more detail the accuracy of calculating the 1D distribution, over magnetic flux surfaces, of the net radiated power density, $P_{EC}(\rho)$, which allows for the emission and absorption of EC waves, and their reflection from the vacuum chamber wall. To this end, very recently a comparison [2] of numeric codes SNECTR [3], CYTRAN [4], CYNEQ [5] and EXACTEC [6] was carried out for different electron temperature profiles and average temperatures of relevance for fusion reactor-grade magnetoplasmas. A comparison of results was made for the following cases:

(A) *specular* reflection of the EC waves from the wall of the vacuum vessel, a *cylinder* with *circular* cross-section (EXACTEC and SNECTR),

(B) (i) *diffuse* reflection in a *circular cylinder* (SNECTR),
(ii) *diffuse* reflection in *any* geometry or *any* reflection in a *noncircular toroid* (CYTRAN and CYNEQ, based on the assumption [4] of the angle isotropy of the radiation intensity, which has been suggested by the results from SNECTR for these cases, especially for diffuse reflection in noncircular toroids, see [3,4]).

The benchmarking [2] has shown good agreement of results within the cases A and B. The results [2] have confirmed the expectation that for large enough reflectivity of the vacuum vessel wall, R_w (>~0.5), the cases A and B provide, respectively, the lower and upper bounds for $P_{EC}(\rho)$, including that for the modulus of $P_{EC}(\rho)$, inverted in sign in the plasma column periphery because of the net self-heating of the plasma by EC waves in the periphery. This

expectation was based on the fact that either the diffuse reflection or the noncircular toroidal geometry make

(*) the trajectories of the waves distributed more homogeneously over the plasma volume,

(**) the radiation intensity more isotropic in the wave direction angles,

as compared with the case of specular reflection in a circular cylinder. The above homogenization and isotropisation of radiation intensity are valid for radiation frequencies for which the mean free path of the waves is comparable with, or exceeds, the plasma column diameter, while these frequencies appear to be responsible for the dominant contribution to $P_{EC}(\rho)$ for large enough R_w (see [3-6]). In the case A, the radiation from the hot plasma core is reflected from the wall back and, hence, its re-absorption in the core is higher, as compared with the case B. In the latter case, the radiation from the hot plasma core travels longer in a colder periphery and is absorbed there stronger, giving a stronger reversal of $P_{EC}(\rho)$.

Here we extend this analysis to show the following approximate scaling laws on the example of calculations with CYNEQ: (i) new simple formula for the volume-integrated EC power loss, P_{EC}^{tot} (Sec. 2); (ii) universal shape of the $P_{EC}(\rho)$ profile: namely, the normalized profile, $P_{EC}(\rho)/P_{EC}^{tot}$, appears to be very close for identical normalized temperature profiles, $T_e(\rho)/\langle T_e\rangle$ and substantially different volume-averaged temperatures, $\langle T_e\rangle$; this suggests the possibility of characterizing the accuracy of various numeric codes (Sec. 3); and (iii) in the central part of plasma, profile $P_{EC}(\rho)$ in the case A may be close enough to that in the case B for larger value of R_w, that suggests introduction of an effective R_w, incorporating the type of reflection (diffusive or specular) and the geometry of the vacuum chamber (Sec. 4).

2. New Formula for Volume-Integrated EC Power Loss in Tokamaks

The first successful attempt to suggest a fitting formula, which describes numerical results for the volume-integrated EC power loss, P_{EC}^{tot}, in fusion reactor-grade plasmas, was done by Trubnikov [7] for *homogeneous* electron density n_e and temperature T_e (the accuracy of Trubnikov's formula is ~50% in the range $5< T_e <100$ keV [7]; for the survey of subsequent variations/improvements see the survey [8]). Similar task for a wide class of *inhomogeneous* n_e and T_e profiles, defined by

$$T_e(\rho) = T_e(1) + \left(T_e(0) - T_e(1)\right)\left[1-\rho^{\beta_T}\right]^{\gamma_T}, \quad (1)$$

$$n_e(\rho) = n_e(1) + \left(n_e(0) - n_e(1)\right)\left[1-\rho^{\beta_n}\right]^{\gamma_n}, \quad (2)$$

(for $\beta_n=2$) was fulfilled in [9] (first formula on page 674) via fitting (with an accuracy less than 10%) the results of direct numerical integration along EC wave path in toroidal geometry without wave's reflection from the walls ($R_w=0$) and using the scaling law $(1-R_w)^{1/2}$, suggested in [7] for a cylinder and verified in [3] for a toroid. The treatment [9] extended the similar work [10] where both β_n and β_T were fixed (see Eq. (15) in [10]). However, the presence of particular parameters (β_T, γ_T, γ_n, in [9] and γ_T, γ_n in [10]) requires solving an inverse problem of their reconstruction in the case when n_e and T_e profiles do not belong to the class of Eqs. (1),(2).

To avoid this difficulty we propose a new formula which fits the numerical results from CYNEQ and gives a simplest extension of the formula [7] to the case of n_e and T_e profiles expected for fusion reactor-grade tokamaks (ITER and DEMO):

$$P_{EC}^{tot} = 4.14\cdot 10^{-7}\,\frac{\sqrt{n_e^{(eff)}}\left(T_e^{(eff)}\right)^{2.5} B_0{}^{2.5}\sqrt{1-R_W}}{\sqrt{a_{eff}}}\left(1+2.5\frac{T_e^{(eff)}}{511}\right)V,\ \ [MW], \qquad (3)$$

where the effective temperature $T_e^{(eff)}$ differs from the volume-averaged temperature, while effective density coincides with the volume-averaged density,

$$T_e^{(eff)} = \int_0^1 T_e(\rho)d\rho \neq \langle T_e\rangle \equiv 2\int_0^1 T_e(\rho)\,\rho\, d\rho\ , \qquad n_e^{(eff)} = \langle n_e\rangle\ . \qquad (4)$$

In Eq. (3), the density is in 10^{20} m-3, temperature, in keV; $V = 2\pi R\,\pi a_{eff}^2$ is plasma volume; major, *R*, and *effective* minor radius, allowing for elongation *k*, $a_{eff}=a\cdot(k)^{1/2}$, are in meters; magnetic field on axis, B_0, in Tesla. Here, the calculations of CYNEQ are carried out assuming that the profile of *total* magnetic field, averaged over magnetic surface, is flat, that, e.g., for ITER "inductive" regime is accurate to <20% [11]: $B_{tot}(\rho)=B_T(0)\equiv B_0$. Formula (3) coincides with the result [7] for a homogeneous T_e and n_e profiles if one uses Trubnikov's transparency factor and takes the weakly relativistic expression for the volumetric (i.e. fully transparent) total EC power loss.

A comparison of absolute values and relative deviations of formula (3) and formula [9] from CYNEQ's results is carried our for various temperature profiles given in Table I. Most of major parameters are taken close to ITER case: *R*=6.2 m, a_{eff}=2 m, B_0.=5.3 T, $R_W = 0.6$, $n_e(0) = 1\cdot 10^{20}\ m^{-3}$, $n_e(1) = 0.5\cdot 10^{20}\ m^{-3}$, $\beta_n = 2, \gamma_n = 0.1$. The results are presented in Figure 1. Note that we compare with formula [9] for elongation *k=1* (this corresponds to neglecting some deviation of this formula from the dependence on *a* and *k* via the unified parameter a_{eff}). The ITB-profile designates a profile which is steeper than the "advanced" T_e profile and is close enough to the case of the observed internal transport barriers.

TABLE I: PARAMETERS OF TEMPERATURE PROFILES

Profile number		1	2	3	4	5	6	7	8	9	10	11	12	13	14	15	16	17	18	19	20	21	22	23	24
T_e, keV	$T_e(0)$	20	30	40	50	20	30	40	50	20	30	40	50	20	30	40	50	20	30	40	50	20	30	40	50
	$T_e(1)$	2				0.01				2				0.01				2				0.01			
Profile type		parabolic with pedestal				parabolic without pedestal				ITB-profile with pedestal				ITB-profile without pedestal				advanced with pedestal				advanced without pedestal			
		γ_T =1.5, β_T =2								γ_T =16.1, β_T =9.3								γ_T =8, β_T =5.4							

It is seen that for the cases of most practical interest for a fusion reactor, namely profiles with a pedestal, the deviation is less than 25%. (Note that, e.g., for the regimes 1-4 taking $T_e^{(eff)}$ = $\langle T_e\rangle$ in Eq. (3) gives the ~40% underestimate of CYNEQ's results.) Also, formula [9] shows good agreement with the results from CYNEQ for T_e profiles of Table I.

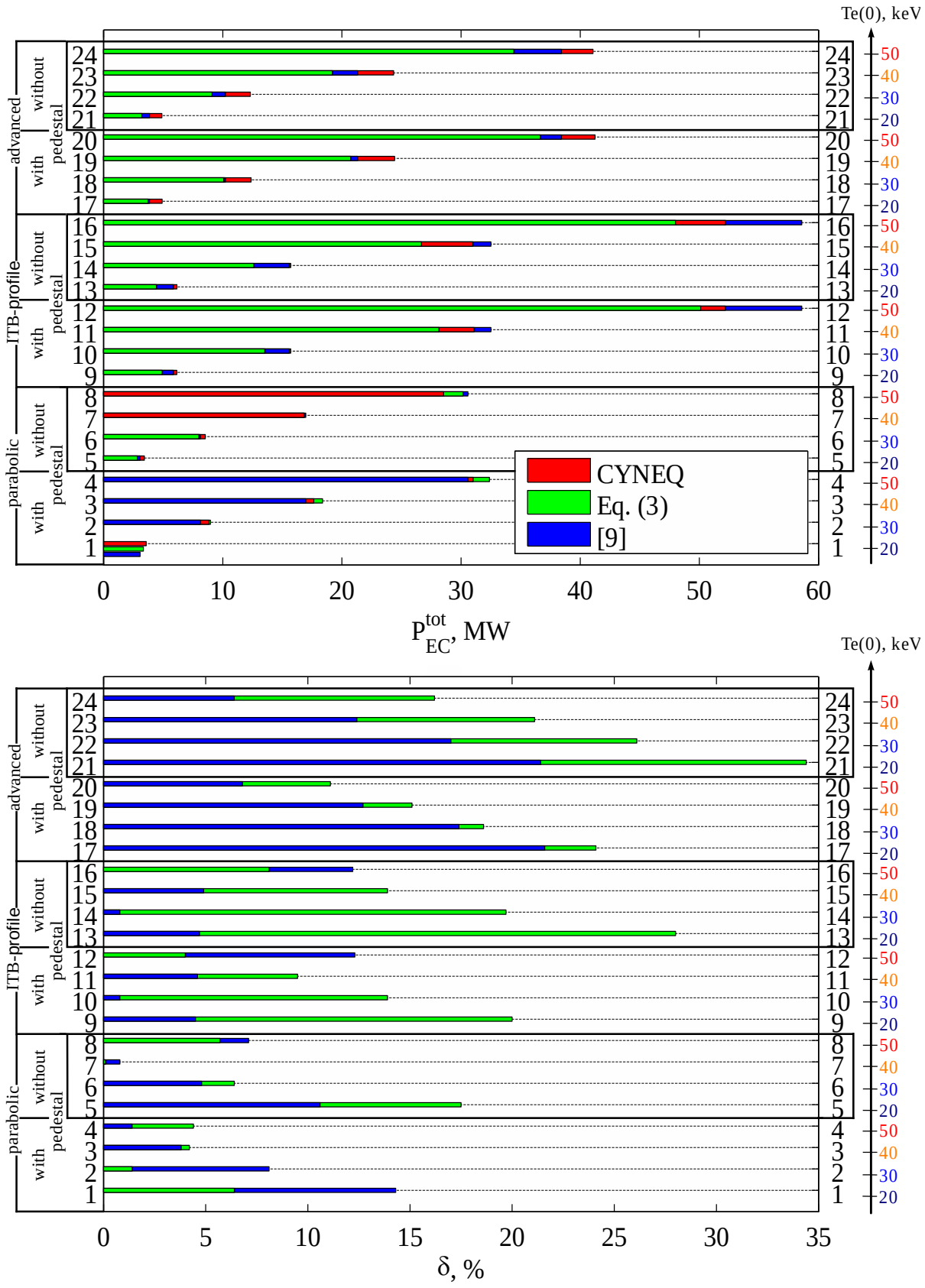

FIG. 1. Upper: comparison of EC total power loss, calculated with CYNEQ, formula (3) and formula [9] (first formula on page 674), for temperature profiles from Table I. Lower: relative deviations of these formulae from CYNEQ's results, $\delta = \left| P_{EC}^{tot} / P_{EC}^{tot,CYNEQ} - 1 \right| \cdot 100\%$.

3. Universal Shape of Spatial Profile of Power Loss

The shape of the $P_{EC}(\rho)$ profile is defined as a normalized profile, $P_{EC}(\rho)/P_{EC}^{tot}$, where P_{EC}^{tot} is the volume-integrated EC power loss, while the shapes of electron density and temperature profiles are defined, respectively, as $n_e(\rho)/\langle n_e\rangle$ and $T_e(\rho)/\langle T_e\rangle$, where $\langle\ \rangle$ denotes volume-averaging.

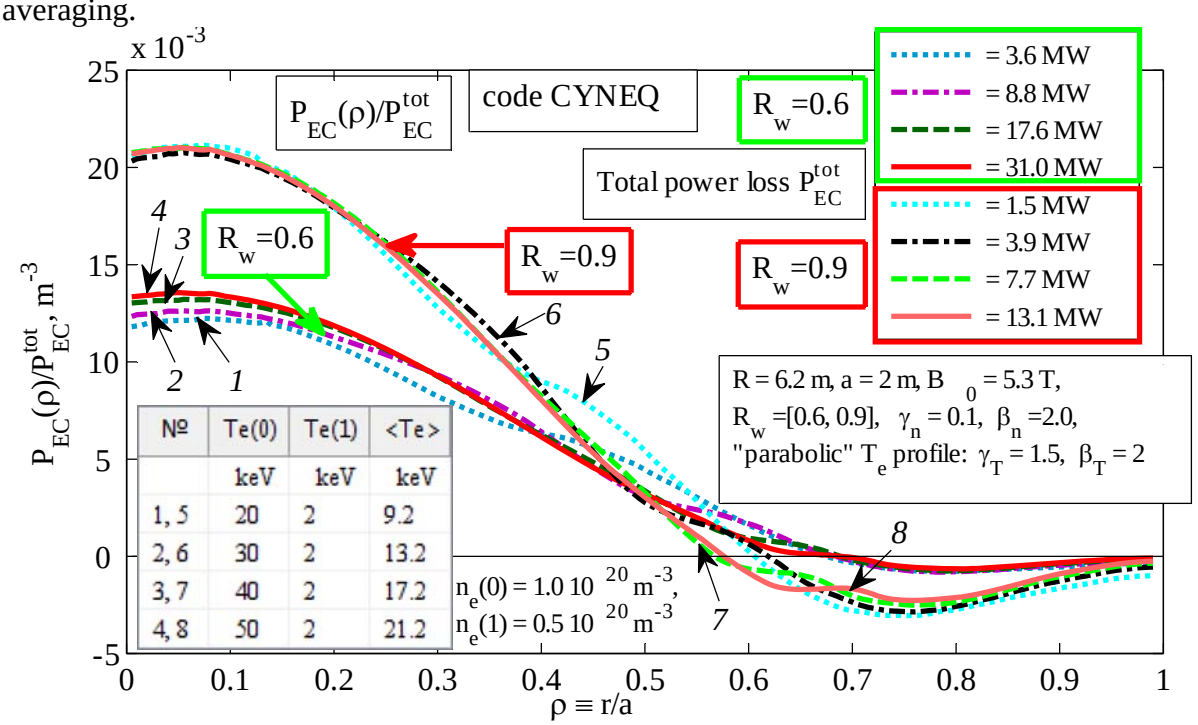

FIG. 2. The normalized profiles of the net radiated power, $P_{EC}(\rho)/P_{EC}^{tot}$, for different values of volume-averaged temperature, $\langle T_e\rangle$, and identical shapes of temperature profile, $T_e(\rho)/\langle T_e\rangle$, for the case of parabolic T_e profile with a pedestal and wall reflectivity R_w = 0.6 and 0.9.

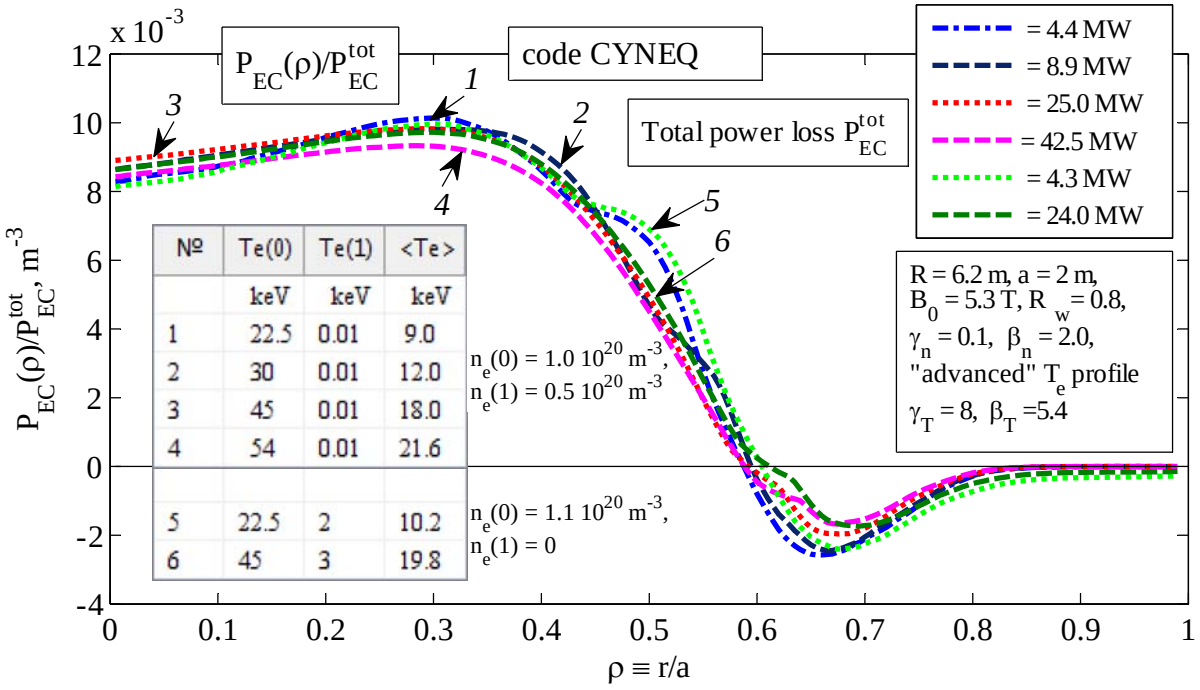

FIG. 3. The same as in FIG. 2, but for the "advanced" T_e profile (with and without pedestal), wall reflectivity R_w = 0.8, and two slightly different n_e profiles.

Figures 2,3 give a comparison of the normalized profiles for two different shapes of temperature profile (parabolic and "advanced") and three values of wall reflectivity. It is seen that the shape of the $P_{EC}(\rho)$ profiles for identical shape of temperature profile, $T_e(\rho)/\langle T_e \rangle$, appears to be very close for substantially different values of volume-averaged temperature, $\langle T_e \rangle$.

The degree of similarity of normalized profiles appears to quantify the accuracy of basic approximations used in CYNEQ because these (namely, isotropy of the radiation intensity, spatial homogeneity of intensity in the optically thin (outer) region, rather weak sensitivity of $P_{EC}(\rho)$ to the definition of the boundary of this region in the $\{\rho,\omega\}$-space) work better for higher R_w and not so steep profiles of plasma temperature and density. It is seen that in the plasma center the similarity is better for higher R_w, whereas in the region ρ=0.3-0.7, where CYNEQ is less accurate, the similarity is worse for all the values of R_w (Figure 4). Note that the decrease of CYNEQ's accuracy in this region stems from the interpolation procedure between the optically thick core and the optically thin outer layer (which covers the entire plasma volume for a substantial part of frequency range responsible for major contribution to $P_{EC}(\rho)$, see Figs. 1,2 in [12]). This procedure is used in CYNEQ as an alternative to evaluation of the contribution of the optically thick core in CYTRAN [4] because the latter procedure formally gives a divergence of $P_{EC}(\rho)$ at ρ=0 and may overestimate $P_{EC}(\rho)$ in the central plasma.

The above suggests the possibility of characterizing the accuracy of various numeric codes via comparing the universality of the shape of the $P_{EC}(\rho)$ profiles.

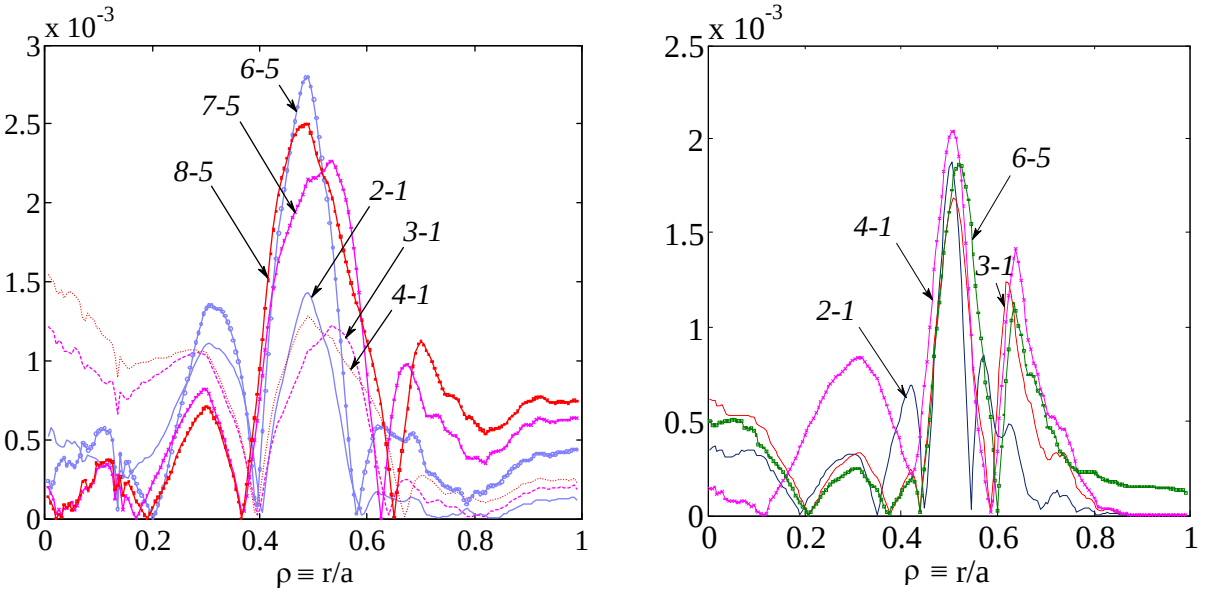

FIG. 4. The absolute value of the difference of the normalized profiles, obtained (for identical shapes of T_e and n_e, and equal values of R_w) by subtraction of the profile with the minimal $\langle T_e \rangle$. The difference of numbers in the curve's labels corresponds to the difference of curves with respective numbers in Figure 2 (left) and Figure 3 (right).

4. An Effective Wall Reflection Coefficient

The comparison of the results within two cases, A and B (as defined in Sec.1), enabled the authors [2] to prove these cases to provide, respectively, the lower and upper bounds for $P_{EC}(\rho)$, including that for the modulus of $P_{EC}(\rho)$, inverted in sign in the plasma column periphery. The difference of these cases is caused by the various types of heat transfer (or, equivalently, various distribution the EC wave ray trajectories over plasma volume) under condition of the dominance of heat transfer at those radiation frequencies for which the mean free path of EC waves, as shown in [3-6], is comparable with, or longer than, the plasma effective minor radius. Indeed, in the case A, one has direct interaction of the hot center with the wall, because the rays from hot center return back from the wall after specular reflection in a circular cylinder with a minimal loss of energy in the periphery, whereas in the case B, because of diffuse reflection from the wall or of the geometry (toroid with non-circular cross-section), the ray from the hot center travels in the periphery (and heats it) as much as possible before coming back to the center. Besides causing the above-mentioned difference of the absolute values of the $P_{EC}(\rho)$ profile, these features of heat transfer allow to indicate another quantitative link of the cases A and B: the hot center may "see" the wall with an effective coefficient of reflection which incorporates the type of reflection (diffusive or specular) and the geometry of the vacuum chamber. The best way to illustrate this feature is to take a steep T_e profile with more or less uniform plateau in the center. This is the case for the "advanced" T_e profile. Figure 5 gives a solution of the inverse problem of reconstructing the value of the wall reflectivity R_w for which in the central part of plasma the profile $P_{EC}(\rho)$, calculated with CYNEQ, coincides with the available result from EXACTEC for a given, obviously smaller value of R_w.

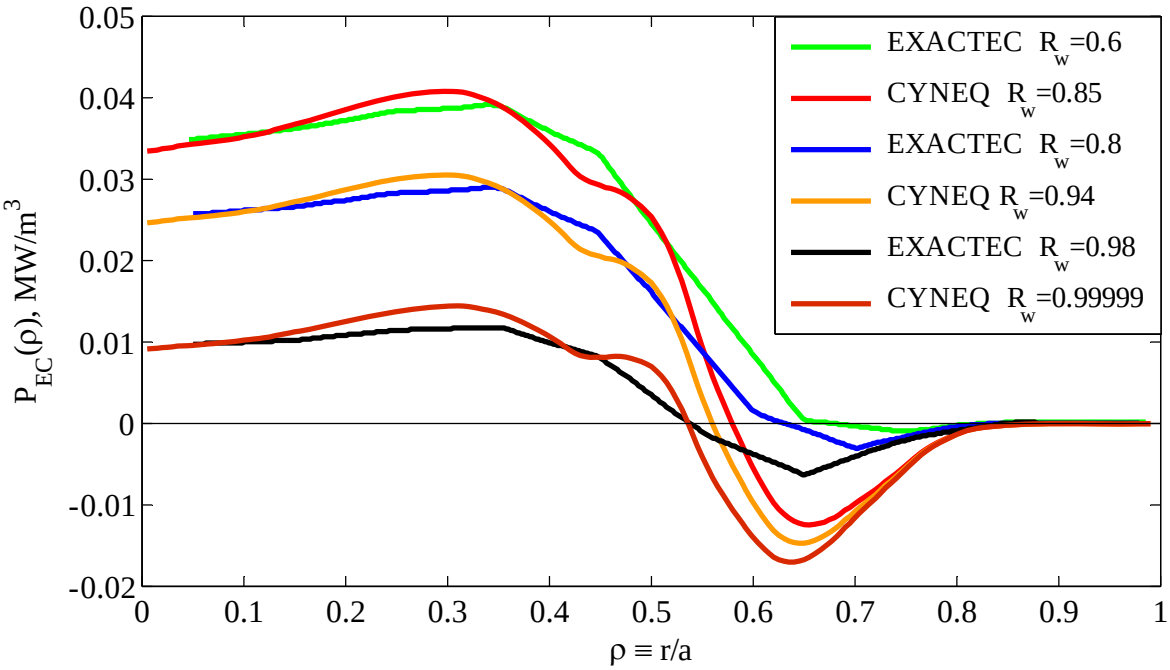

FIG. 5. Approximate coincidence of the $P_{EC}(\rho)$ profiles in the central plasma, calculated with the codes EXACTEC (the curves are taken from Fig. 3 in [6]) and CYNEQ, for the "advanced" T_e profile (and other conditions of the curve 1 in Figure 3 herein) and different values of wall reflectivity R_w.

5. Conclusions

(a) A new formula, Eq. (3), is proposed which fits the numerical results from the code CYNEQ [5] for a wide range of T_e profiles (for profiles with a pedestal, with an accuracy less than ~25%) and gives a simplest extension of the Trubnikov's formula [7] to the case of n_e and T_e profiles expected for fusion reactor-grade tokamaks. This formula does not assume analytic representation of T_e and n_e profiles (e.g., in the form of Eqs. (1),(2)).

(b) A universality of the shape of the $P_{EC}(\rho)$ profile is found: the normalized profile, $P_{EC}(\rho)/P_{EC}^{tot}$, for *identical* normalized temperature profiles, $T_e(\rho)/\langle T_e \rangle$, appears to be very close for substantially *different* volume-averaged temperatures, $\langle T_e \rangle$. The correlation of the degree of such a similarity with the accuracy of the code CYNEQ suggests the possibility of characterizing the accuracy of various numeric codes.

(c) It is possible to introduce an effective coefficient of wave's reflection from the wall to incorporate the type of reflection (diffusive or specular) and the geometry of the vacuum chamber (e.g., circular cylinder or noncircular toroid): in the central plasma, $P_{EC}(\rho)$ in the case A (see Sec.1) may be close enough to that in the case B for a larger value of reflectivity.

Acknowledgements. This work is partly supported by the Russian Federal Program of Support to Leading Scientific Schools (grant NSh-2457.2008.2). A part of this work was carried out by A.B.K. during the fellowship of the Cariplo Foundation (the Landau Network-Centro Volta). A.B.K. is grateful to the coauthors of the paper [2] for helpful discussions. Participation of A.B.K. in the 22nd IAEA Fusion Energy Conference is partly supported by the travel grant from the IAEA.

REFERENCES

[1] ALBAJAR, F., BORNATICI, M., CORTES, G., et al., Nucl. Fusion **45** (2005) 642.
[2] ALBAJAR, F., BORNATICI, M., ENGELMANN, F., KUKUSHKIN, A.B., "Benchmarking of codes for calculating local net EC power losses in fusion plasmas" (Proc. EC-15 workshop, USA, March 2008; an extended version will be published in Fusion Sci. & Technol., January 2009).
[3] TAMOR, S., Fusion Technol. **3** (1983) 293; Nucl. Instrum. Methods Phys. Res. **A271** (1988) 37.
[4] TAMOR, S., "A simple fast routine for computation of energy transport by synchrotron radiation in tokamaks and similar geometries", Report SAI-023-81-189-LJ/LAPS-72 (La Jolla, CA: Science Applications), 1981.
[5] KUKUSHKIN, A.B., Proc. 14th IAEA Conf. on Plasma Phys. & Contr. Fusion, Wuerzburg, 1992, v. 2, pp. 35-45; CHEREPANOV, K.V., KUKUSHKIN, A.B., Proc. 20th IAEA Fusion Energy Conference. (Vilamoura, Portugal, 2004), TH/P6-56.
[6] ALBAJAR, F., BORNATICI, M., ENGELMANN, F., Nucl. Fusion **42** (2002) 670.
[7] TRUBNIKOV, B.A., in Reviews of Plasma Physics, vol. 7 (M.A. Leontovich, Ed.). New-York: Consultants Bureau, 1979, p. 345.
[8] BORNATICI, CANO, R., DE BARBIERI, O., ENGELMANN, F., Nucl. Fusion **23** (1983) 1153.
[9] ALBAJAR, F., JOHNER, J., GRANATA, G., Nucl. Fusion, **41** (2001) 665.
[10] FIDONE, I., MEYER, R.L., GIRUZZI, G., GRANATA, G., Phys. Fluids B **4** (1992) 4051.
[11] POLEVOI, A.R., MEDVEDEV, S.YU., MUKHOVATOV, S.V., et al., J Plasma Fusion Res. SERIES, **5** (2002) 82-87.
[12] CHEREPANOV, K.V., KUKUSHKIN, A.B., MINASHIN, P.V., NEVEROV, V.S. Proc. 34th EPS Conf. Plasma Phys. (Warsaw, July 2007), ECA, vol. 31F, P-4.133.